New Photocycle Intermediates in the Photoactive Yellow Protein from *Ectothiorhodospira halophila*: Picosecond Transient Absorption Spectroscopy

L. Ujj,* S. Devanathan,# T. E. Meyer,# M. A. Cusanovich,# G. Tollin,# and G. H. Atkinson*
*Department of Chemistry and Optical Science Center, and #Department of Biochemistry, University of Arizona, Tucson, Arizona 85721 USA

ABSTRACT Previous studies have shown that the room temperature photocycle of the photoactive yellow protein (PYP) from *Ectothiorhodospira halophila* involves at least two intermediate species: I_1, which forms in $<$10 ns and decays with a 200-μs lifetime to I_2, which itself subsequently returns to the ground state with a 140-ms time constant at pH 7 (Genick et al. 1997. *Biochemistry.* 36:8–14). Picosecond transient absorption spectroscopy has been used here to reveal a photophysical relaxation process (stimulated emission) and photochemical intermediates in the PYP photocycle that have not been reported previously. The first new intermediate (I_0) exhibits maximum absorption at $\sim$510 nm and appears in $\leq$3 ps after 452 nm excitation (5 ps pulse width) of PYP. Kinetic analysis shows that I_0 decays with a 220 $\pm$ 20 ps lifetime, forming another intermediate ($I^{\ddagger}_0$) that has a similar difference wavelength maximum, but with lower absorptivity. $I^{\ddagger}_0$ decays with a 3 $\pm$ 0.15 ns time constant to form I_1. Stimulated emission from an excited electronic state of PYP is observed both within the 4–6-ps cross-correlation times used in this work, and with a 16-ps delay for all probe wavelengths throughout the 426–525-nm region studied. These transient absorption and emission data provide a more detailed understanding of the mechanistic dynamics occurring during the PYP photocycle.

INTRODUCTION

The photoactive yellow protein (PYP) from *Ectothiorhodospira halophila* is a small (14 kDa), water-soluble, cytoplasmic protein that is also found in several other halophilic purple phototrophic bacteria (Meyer, 1985; Meyer et al., 1987, 1990). The bright yellow color of PYP arises from a single, broad (60 nm) absorption band with a maximum at 446 nm ($\epsilon = 45\ \mathrm{mM}^{-1}\ \mathrm{cm}^{-1}$; cf. Fig. 1). PYP is thought to function biochemically as an initiator of negative phototaxis (Sprenger et al., 1993), although this has not been conclusively established. Photoactivity in PYP at room temperature is manifested by a photocycle that is initiated by excitation into its 446-nm absorption band. The radiative lifetime of the PYP excited electronic state (PYP*) has been reported to be $\sim$12 ps from fluorescence decay measurements (480 nm excitation) (Meyer et al., 1991), although global analysis of the decay curves also showed additional slower decay processes. More recent measurements by Chosrowjan et al. (1997) have found two main fluorescence decay components with time constants ranging from 700 $\pm$ 200 fs to 7 $\pm$ 3 ps.

The chromophore of PYP is a *p*-hydroxycinnamyl cysteine thioester (Baca et al., 1994; Hoff et al., 1994; Kort et al., 1996) that undergoes *trans-cis* photoisomerization around its only carbon-carbon double bond (Fig. 2) (Genick et al., 1997a). Previous transient absorption studies using 10-ns time resolution concluded that the PYP photocycle comprises only two intermediates (Meyer et al., 1987, 1989; Hoff et al., 1994). The first intermediate, referred to as I_1, has a red-shifted absorption maximum relative to ground-state PYP ($\epsilon_{rel} = 0.50$) and appears in $<$10 ns after 446-nm excitation. The second intermediate, referred to as I_2, has a blue-shifted absorption maximum relative to PYP ($\epsilon_{rel} = 0.4$), and is formed from I_1 with a time constant of 200 μs. I_2 decays to ground-state PYP with a lifetime of 140 ms. The rates of formation of I_2 and its decay to ground state are affected by solvent and pH (Meyer et al., 1989; Genick et al., 1997b). Results from steady-state, low-temperature optical spectroscopy suggest that the PYP photocycle may contain additional long-wavelength intermediates (490 nm; Hoff et al., 1992; Imamoto et al., 1996), but in the absence of kinetic studies with higher time resolution, it is difficult to distinguish low-temperature artifacts from actual room temperature PYP photocycle intermediates. In the present study, picosecond transient absorption (PTA) data have been measured at room temperature after 452-nm excitation of PYP. These reveal the presence of two new picosecond photochemical intermediates, along with stimulated emission from electronically excited PYP occurring over a time period as long as 16 ps.

Received for publication 12 December 1997 and in final form 9 April 1998.
Address reprint requests to Dr. George H. Atkinson, Department of Chemistry, University of Arizona, Tucson, AZ 85721. Tel.: 520-621-6293; Fax: 520-621-4858; E-mail: Atkinson@ccit.arizona.edu; or Dr. Gordon Tollin, Department of Biochemistry, University of Arizona, Tucson, AZ 85721. Tel.: 520-621-3447; Fax: 520-621-9288; E-mail: gtollin@u.arizona.edu.

0006-3495/98/07/406/07 $2.00

EXPERIMENTAL

Materials

Recombinant PYP was prepared by the procedure reported by Genick et al. (1997b). Twenty-five milliliters of a 2.6 OD/cm solution in 20 mM Tris-Cl buffer at pH 7.0 was used for these experiments.

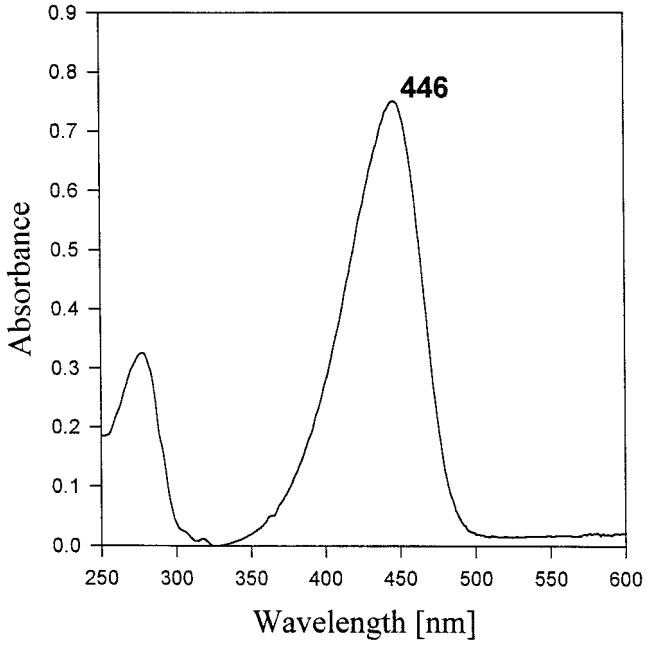

FIGURE 1 Absorption spectrum of PYP in HEPES buffer, pH 7.0.

Instrumental methods

The instrumentation and experimental procedures used to record PTA traces from retinal proteins such as bacteriorhodopsin and rhodopsin have been described in detail elsewhere (Brack et al., 1993; Delaney et al., 1995; Popp et al., 1995; Ujj et al., 1996). Several modifications of the laser system and of the procedures were used in the PYP experiments described here. The modified instrumentation contains two cavity-dumped dye lasers, each of which was synchronously pumped (76 MHz pulse train with 30 ps duration (FWHM)) by the frequency-tripled (351 nm) output of a mode-locked Nd:YLF laser (Coherent Antares). The 1.2-W pump power at 351 nm was divided about equally into two parts by a polarization beam splitter. The power ratio between the two pump beams was adjusted with a half-lambda plate. The power available to pump each dye laser ($>$1.5 times threshold) maintained the stable spectral and temporal properties of the laser pulses for the several hours needed to complete a set of PTA measurements. Both dye lasers were operated at 400-kHz repetition rates through the use of separate cavity dumpers, each of which was electronically synchronized to the Nd:YLF mode locker.

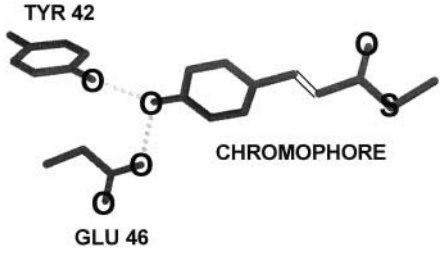

FIGURE 2 Structure of the chromophore bound to Cys^{69} in PYP. Also shown is the location of the double bond that is photoisomerized during the photocycle, and the hydrogen bonding network that connects the phenolic oxygen of the chromophore to nearby active site residues in the PYP ground state (coordinates from Borgstahl et al., 1995).

The 452-nm wavelength (3 nJ/pulse), 3-ps pulse width of the pump laser used to initiate the PYP photoreaction was obtained using a stilbene dye. The probe laser was scanned through the 420–535-nm spectral region to record PTA traces at selected wavelengths. Coumarin 500 and 480 dyes, together with stilbene dyes, were used to cover this spectral region. The temporal width of the probe laser pulses ranged between 3 ps and 6 ps, because of the different alignment and pumping conditions required to maintain the laser operation at ~100-nm bandwidths. The auto- and cross-correlation times (CCT) were measured for each set of laser pulses with a commercial correlator (model FR-103XL; Femtocrome Research). The resultant timing jitter measured for the two probe dye laser pulses was typically $<$2 ps.

PTA traces were recorded with phase-sensitive techniques (lock-in amplifiers) and photodiode detectors (model PD100; EG&G). Procedurally, two different methods were used to elucidate the time and wavelength dependence of the absorbance/transmittance changes observed in the PYP photoreaction:

1. Absorbance changes were recorded at electronically fixed time delays (100 ps and 26 ns) over the 420–535-nm spectral region spanned by the probe laser pulses. At the 26-ns time delay, presumably only the I_1 intermediate is present (Meyer et al., 1987).

2. PTA traces, with probe laser pulses at selected wavelengths, were recorded continuously as a function of delay time (between −50 ps and 200 ps, with 1-ps time resolution and between −100 ps and 4 ns with 25-ps time resolution). Optical delay lines were used to control time delays. PTA data at 26-ns, 52-ns, and 78-ns time delays were measured independently, using electronic time delays via control of the cavity dumpers. All such PTA traces were normalized to the relative absorbance changes observed for the fixed time delays used in method 1 above.

All PTA data reported here were obtained from a single PYP sample (25 ml of 2.6 OD/cm at 446 nm). The PYP solution was examined at 17°C as flowing (~12 m/s), plane-parallel, liquid jets (~400-μm diameter) to avoid photodegradation. Complete replacement of the PYP sample volume between successive sets of laser pulses occurred within the 2.5-μs interval (400-kHz repetition rate of both lasers). The adequacy of these parameters in completely replacing the sample volume measured between pairs of laser pulses was established by increasing the repetition rates of both the pump and probe lasers (e.g., to 1 MHz) with the same flow speed of the sample.

Optical absorption spectra recorded from the PYP sample before and after each set of PTA measurements showed that no significant change in the PYP concentration had occurred. Nanosecond transient photolysis measurements (Meyer et al., 1987, 1989; Genick et al., 1997b) performed

before and after each measurement also showed no degradation of the PYP photocycle.

Quantitative kinetic analysis

The time-dependent absorbance traces, measured at eight different wavelengths (Fig. 3), were analyzed in terms of a global kinetic fit spanning the time interval from −100 ps to 100 ns (4–6 ps CCT). This analysis methodology has the advantage that the function used is independent of the assumed kinetic model. The model function itself comprises the sum of five exponential terms convoluted with the cross-correlation function (normalized to 1) representing the pump and probe laser pulses. It assumes that the pump laser pulses do not cause a significant concentration change in PYP or introduce saturation effects (a linear dependence of absorbance change amplitudes on pump power was observed; see below), and that the probe laser pulses do not significantly perturb the photoreaction (although probe pulses shorten the effective lifetime of PYP* via stimulated emission; see below). The nonperturbation of probe pulses can be rationalized in terms of their extremely low power (<150 fJ in each 4-ps pulse). Based on these criteria, time constant values obtained in the analysis that are less than the CCT may be overestimated.

The specific nonlinear Levenberg-Marquart method (Press et al., 1986) that was employed minimized the χ^2 estimation of error by varying both the amplitudes and time constants of each exponential term. The fit was computed with Microcal Origin 5.0. Although the overall global fits must satisfy all of the PTA data, procedurally the PTA traces recorded on the picosecond time scale were fitted together, followed by the execution of a fit to the PTA traces recorded on the nanosecond time scale. Statistical errors were calculated by taking into account all errors associated with the parameters used for the measurements (e.g., pump and probe power; signal amplitudes). Additional systematic errors in the 440-nm region could be introduced by different alignment procedures (i.e., beam overlap).

The quantitative characteristics of these measurements were validated in two ways. First, the absorbance signal was found to be linearly (>95% confidence level) dependent on the pump power over the range of 0.5–3 mW (i.e., 1.25–7.5 nJ/pulse) at both 100-ps and 26-ns time delays (the beam waist of the pump laser within the sample was ~20 μm). Thus the 3 nJ/pulse excitation energy selected to record all of the data presented herein was within this linear range. Second, no effects attributable to systematic exposure of the sample to the pump and probe laser pulses were found. Absorbance changes were recorded both with and without

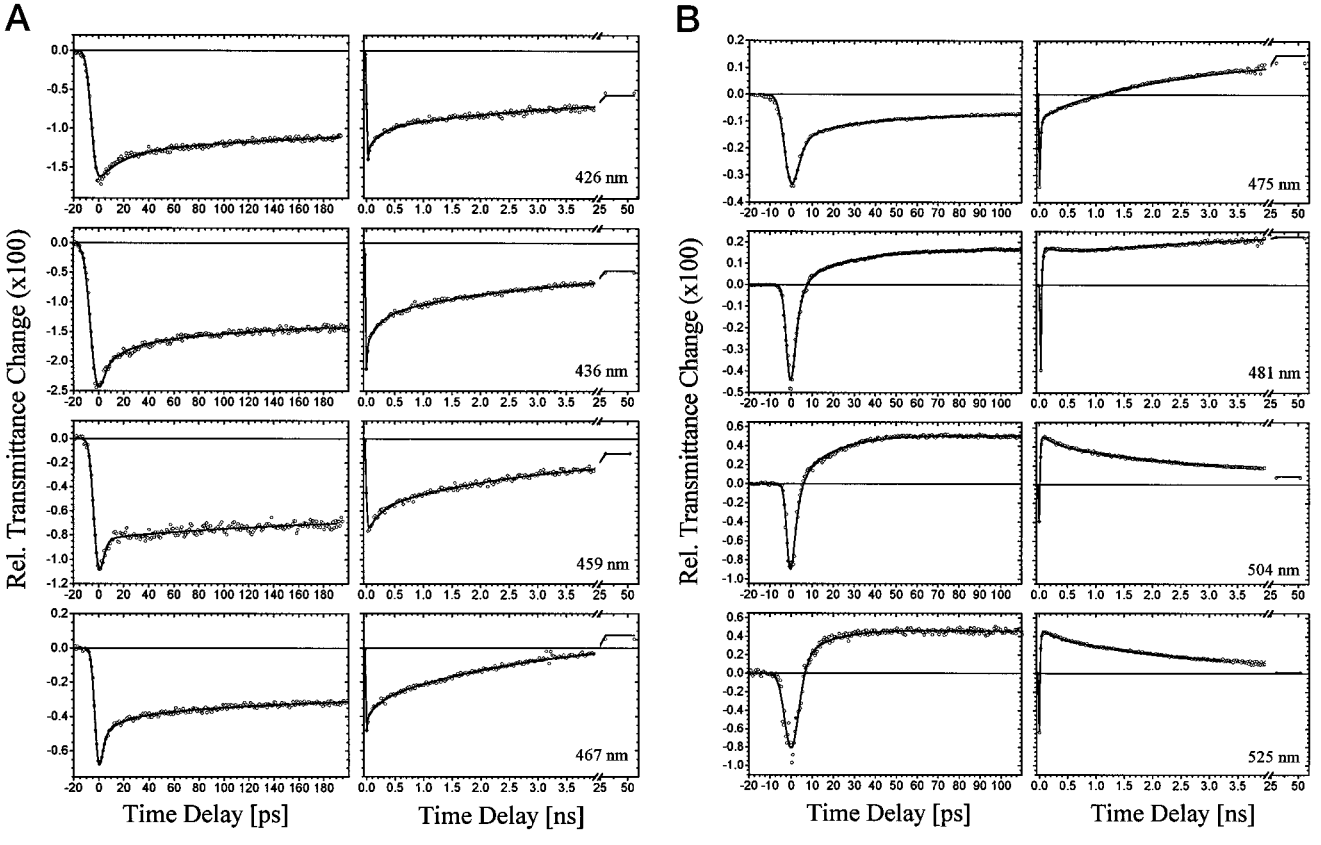

FIGURE 3 PTA traces obtained for eight wavelengths. (*A*) 426, 436, 459, and 467 nm. (*B*) 475, 481, 504, and 525 nm. Time delays of −20 ps to 200 ps are shown in the left panels, and delays out to 50 ns are shown in the right panels. Solid lines correspond to global fit curves (see text for details).

excitation for a variety of pump and probe laser powers, by a series of parallel and sequential data accumulation protocols. Data were measured over three overlapping spectral regions (420–480 nm, 480–510 nm, and 504–535 nm). No systematic effects related to these parameters were observed. No absorbance changes were observed in PTA signals measured at negative time delays (i.e., when the probe pulse arrived at the sample before the pump pulse) when a 12 m/s sample flow rate was used with a 400-kHz repetition rate. These conditions have not been met in previous femtosecond transient absorption (Baltuška et al., 1997) and fluorescence (Chosrowjan et al., 1997) experiments to which these PTA data are compared (see below).

RESULTS

PTA data were recorded for eight different probe wavelengths between 426 nm and 525 nm to obtain the curves presented in Fig. 3. Separate PTA traces were measured for the time regimes between −20 ps and 200 ps (*left panels*) and −20 ps and 6 ns (*right panels*). The 4–6-ps CCT used in these PTA measurements permits time constants as short as 1.5 ps to be confidently extracted through quantitative global fits encompassing all eight sets of PTA data, as described above.

The global fit analysis of these PTA traces (*solid lines* in Fig. 3) demonstrates that two distinct photochemical intermediates not previously reported are present. The I_0 intermediate appears with a ≤3-ps time constant and decays with a 220 ± 20 ps time constant. This kinetic analysis also reveals the presence of a second intermediate $I^{\ddagger}_0$, which is apparent from its 20% lower absorptivity (for example, see the trace in the *right panel* at 481 nm in Fig. 3 *B*) and a greater absorptivity over the ≤490-nm region (Fig. 3 *A*). This species appears with a time constant of ~220 ps and decays with a 3.00 ± 0.15 ns time constant to the previously identified I_1 species (Meyer et al., 1987; Hoff et al., 1994). Difference absorption spectra measured at 100-ps and 26-ns time delays are presented in Fig. 4. The difference spectrum at the 500-ps time delay is taken directly from the traces in Fig. 3.

The absolute absorption spectra for I_0, $I^{\ddagger}_0$, and I_1, corresponding to the differential transmittance changes (Fig. 4), are calculated using known experimental parameters. A critical parameter for the calculation is the extent of conversion of PYP into the photocycle intermediates under the experimental conditions used. Based on the excitation conditions, 30 ± 5% of the PYP is effectively converted to PYP* (Ujj et al., 1996). The ±5% uncertainty in this parameter is due to variation in the laser beam diameters (20–25 μm) in the sample and the overlap conditions of the probe and pump beams (assuming a Gaussian transverse intensity distribution). The I_1 absorption spectrum (Fig. 5) is calculated by adding 6% (corresponding to 20% of 30%) of the PYP ground-state absorbance (see below) to the difference spectrum recorded at 26 ns. This value is obtained

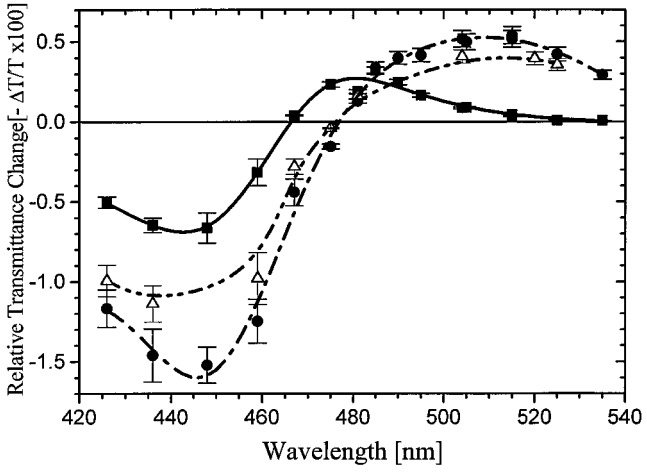

FIGURE 4 Time-resolved difference absorption spectra obtained from PYP at 100 ps (●), 500 ps (△), and 26 ns (■). The continuous lines were obtained by Gaussian fit. The shapes of the lines do not have any physical significance.

from the previously published spectrum of I_1 (Hoff et al., 1994) and the data of Fig. 4, which indicate that 6% of the PYP ground-state population is converted to I_1. The $I^{\ddagger}_0$ absorption spectrum is calculated from the differential transmittance data measured at the 500-ps time delay (Fig. 4) by subtracting a 16% I_1 contribution and adding the same amount of PYP ground-state absorbance. At 500 ps, 84% of the signal is due to absorbance by $I^{\ddagger}_0$. Once the $I^{\ddagger}_0$ absorption spectrum is known, the I_0 spectrum can be calculated from the differential absorption data recorded at the 100-ps time delay. At this latter time delay, 64% I_0 and 34% $I^{\ddagger}_0$ are present. The absolute absorption spectra can also be calculated using the amplitudes of the exponential terms of the kinetic fit results. The two sets of spectra are identical

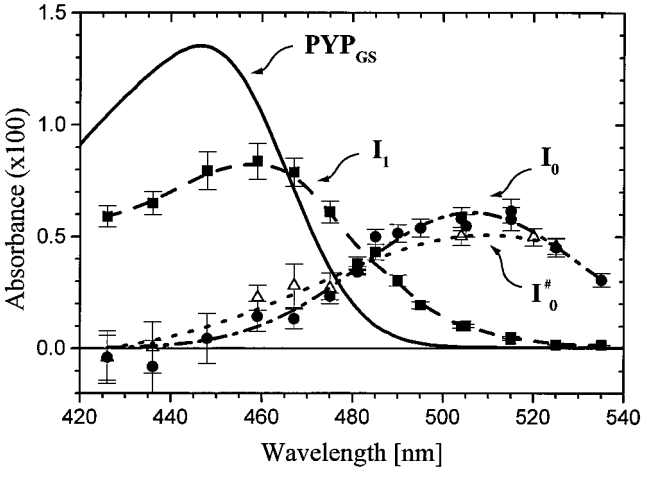

FIGURE 5 Time-resolved absolute absorption spectra calculated for the three intermediates observed in the present experiments, I_0 (≤3 ps) (●), $I^{\ddagger}_0$ (220 ps) (△), and I_1 (3 ns) (■). The ground-state absorption spectrum (——) of PYP is included for comparison. The continuous lines are obtained by using Gaussian functions, although these absorption spectra need not have Gaussian shapes.

within the error limits of the measurements (data not shown).

The absorption spectra in Fig. 5 can be compared to the isosbestic points measured by PTA data recorded at specific time delays. Thus the 100-ps spectrum (representing the ≤3 ps formation/220 ps decay intermediate, I_0) has an isosbestic point with PYP ground state at 476 ± 2 nm (Fig. 5). This isosbestic point corresponds closely to the value of zero absorbance change shown in Fig. 4, a result that supports the validity of the 20% conversion value used for the calculation. The 26-ns spectrum (representing the 3-ns formation/100 μs decay intermediate, I_1) has an isosbestic point at 464 ± 2 nm and a shape analogous to the data reported previously from nanosecond transient absorption studies (Meyer et al., 1987; Hoff et al., 1994), although there is a 5-nm discrepancy between the isosbestic points found in the picosecond versus nanosecond data. Despite this small difference, it is clear that the same intermediate is being observed in all of these experiments.

Stimulated emission from PYP* was also revealed via these PTA data. Within the 4–6-ps CCT, negative PTA signals corresponding to an increase in light intensity reaching the detector were observed for all traces in the 426–525-nm region (Fig. 3, *A* and *B*, and Fig. 6). A time constant for these PTA changes of 1.5 ps was found. For probe wavelengths in the 426–500-nm region, which overlaps the PYP absorption spectrum (Fig. 1), the negative signals occurring within the CCT can be attributed to either bleaching of absorption by the PYP ground state or stimulated emission from PYP*, or both. However, in the 500–525-nm region, where no PYP absorption occurs, the negative signals can be attributed only to stimulated emission. Because the time constants measured throughout the 426–525-nm region remain unchanged (i.e., 1.5 ps), the contribution from bleaching of PYP absorption must be small relative to that due to stimulated emission from PYP*. Such stimulated emission can be detected in these PTA experiments because the emission spatially overlaps the probe laser beam. In addition to these signals, a much smaller (~15%) stimulated emission/bleach signal was observed in the 16-ps time regime (Fig. 6). This must originate from an additional excited state species that is not part of the main photochemical pathway, and whose identity is currently unknown.

It is noteworthy that the transients reported in Baltuška et al. (1997), obtained with 200-fs excitation pulses and probed between 430 and 550 nm, do not explicitly exhibit absorption changes resulting from the formation of the picosecond species observed here, although stimulated emission over this wavelength range with lifetimes of 700 fs and 3.6 ps was obtained. The reasons for this difference are unclear.

DISCUSSION

The 12-ps radiative lifetime measured via room temperature fluorescence from PYP*, together with the low fluorescence quantum yield (~10^{-3}; Meyer et al., 1991), suggests that the PYP photocycle processes occur with high efficiency and that the first photocycle intermediate should be formed in ≤12 ps (cf. also Meyer et al., 1989; Hoff et al., 1992, 1994). These conclusions are generally confirmed by the PTA data presented here, although with somewhat different numerical values. Specifically, the identification of the observed 1.5-ps time constant process with stimulated emission from PYP* (see above), along with the fact that the excitation and probe laser pulses have a CCT of 4–6 ps, leads to the conclusion that the lifetime of PYP* must be ≤3.0 ps. Thus the initial photocycle event observed here (i.e., formation of I_0) would occur within the lifetime of PYP* and, consequently, would have the high quantum yield anticipated for photoactive proteins (Meyer et al., 1989; Hoff et al., 1994). A modified version of the PYP photocycle, which includes the new intermediates observed in these experiments, is presented schematically in Fig. 7.

The PTA data, of course, do not directly provide information on whether the formation of I_0 involves any structural change in the chromophore or in the protein. However, the production of this species probably involves the initial *trans-cis* isomerization of the chromophore (Baca et al.,

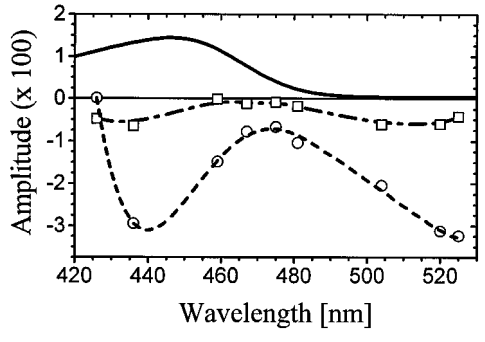

FIGURE 6 Stimulated emission signals (amplitudes from kinetic fits) obtained from the PTA trace. The open circles represent the amplitudes of the ≤3 ps term, and the open squares the 16 ps term of the multiexponential fitting function. The ground-state absorption spectrum of PYP (*solid line in upper panel*) is shown for comparison.

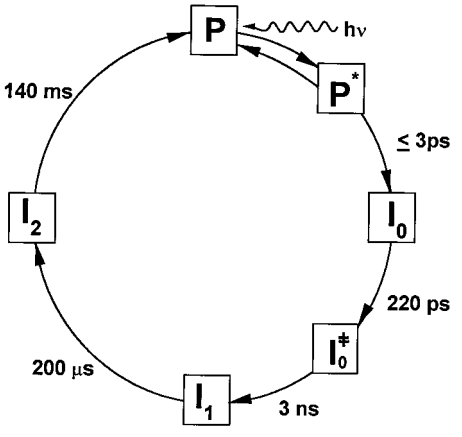

FIGURE 7 Revised photocycle for PYP.

1994; Genick et al., 1997a). The large red shift observed for I_0 and $I^{\ddagger}_0$ relative to ground-state PYP could result from an increase in the negative charge on the phenolic oxygen of the chromophore that occurs when it moves away from the hydrogen-bonding interactions with its active site partners Glu^{46} and Tyr^{42} (Fig. 2) as a result of the absorbed photon. The 220-ps transformation from I_0 to $I^{\ddagger}_0$ can be ascribed to a change in the chromophore/protein interaction that alters the absorptivity (although not the apparent wavelength maximum) of the chromophore spectrum. It is possible that the apparent broadening of the $I^{\ddagger}_0$ spectrum relative to I_0 may result from protein relaxation in the vicinity of the chromophore, which allows other vibrational states of the chromophore to become occupied (Henry et al., 1986). This occurs on a time scale significantly longer than the initial photochemical step and shorter than the transformation to I_1, and thus could be due to protein relaxation processes that involve changes in the hydrogen bond distances due to twisting of the chromophore and reorientation of protein side-chain positions. The 3.0-ns decay of $I^{\ddagger}_0$ to I_1 involves a substantially larger absorption shift to shorter wavelengths. In the present context, this could result from further relaxation of the protein/chromophore system, leading to the establishment of new hydrogen bond interactions (perhaps with Arg^{52}) and, thus, to an additional shifting of the chromophore absorption to shorter wavelengths. Finally, as previously postulated (Meyer et al., 1993), decay of I_1 to I_2 results in a further blue shift as a result of chromophore protonation. This view of the processes involved in the PYP photocycle is obviously speculative. Confirmation of these points requires additional studies, especially ones that utilize time-resolved vibrational spectroscopy.

Previous studies in 67% glycerol at liquid nitrogen temperature (Hoff et al., 1992; Imamoto et al., 1996) revealed the presence of a red-shifted intermediate with a wavelength maximum at 490 nm. It is possible that this intermediate may correspond to either the I_0 or $I^{\ddagger}_0$ species observed near room temperature, although it has been shown that organic solvents (including glycerol) markedly alter the properties of PYP (Meyer et al., 1989). The blue-shifted intermediates observed at low temperatures have not been found at room temperature and may not be part of the normal photocycle. This point deserves further study.

Even though they have quite different chromophores, the retinal proteins rhodopsin and bacteriorhodopsin undergo similar *trans-cis* photoisomerizations and produce red-shifted early intermediates, although on a faster time scale (200–450 fs; Nuss et al., 1985; Schoenlein et al., 1991; Wang et al., 1994). In the case of bacteriorhodopsin, however, the red shift appears to involve charge delocalization between the protonated Schiff base of the retinal chromophore and its counterion (Marti et al., 1991), rather than a change in the hydrogen bond network, as is apparently involved in PYP. It is clear, however, that the sequential pattern of light-induced structural alterations and spectral shifts is similar in the two types of photoactive proteins.

This work was supported in part by grants from the U.S. Air Force Rome Laboratory (F3060295C0100) and the National Science Foundation (MCB-9722781).

REFERENCES

Baca, M., G. E. O. Borgstahl, M. Boissinot, P. M. Burke, D. R. Williams, K. A. Slater, and E. D. Getzoff. 1994. Complete chemical structure of photoactive yellow protein: novel thioester-linked 4-hydroxycinnamyl chromophore and photocycle chemistry. *Biochemistry.* 33: 14369–14377.

Baltuška, A., I. H. M. van Stokkum, A. Kroon, R. Monshouwer, K. J. Hellingwerf, and R. van Grondelle. 1997. The primary events in the photoactivation of yellow protein. *Chem. Phys. Lett.* 270:263–266.

Bogomolni, R. A., and J. L. Spudich. 1991. Archaebacterial rhodopsins: sensory and energy transducing membrane proteins. *In* Sensory Receptors and Signal Transduction. Wiley-Liss, New York. 233–255.

Borgstahl, G. E. O., D. R. Williams, and E. D. Getzoff. 1995. 1.4 Å structure of photoactive yellow protein, a cytosolic photoreceptor: unusual fold, active site, and chromophore. *Biochemistry.* 34:6278–6287.

Brack, T. L., J. K. Delaney, G. H. Atkinson, A. Albeck, M. Sheves, and M. Ottolenghi. 1993. Picosecond time-resolved absorption and fluorescence dynamics in the artificial bacteriorhodopsin pigment BR 6.11. *Biophys. J.* 65:964–972.

Chosrowjan, H., N. Mataga, N. Nakashima, Y. Imamoto, and F. Tokunaga. 1997. Femtosecond-picosecond fluorescence studies on excited state dynamics of photoactive yellow protein from *Ectothiorhodospira halophila. Chem. Phys. Lett.* 270:267–272.

Delaney, J. K., G. H. Atkinson, A. Albeck, M. Sheves, and M. Ottolenghi. 1995. Picosecond time-resolved absorption dynamics in the artificial bacteriorhodopsin pigment 6.9. *J. Phys. Chem.* 99:7801–7805.

Genick, U. K., G. E. O. Borgstahl, K. Ng, Z. Ren, C. Pradervand, P. M. Burke, V. Srajer, T. Teng, W. Schildkamp, D. E. McRee, K. Moffat, and E. D. Getzoff. 1997a. Structure of a protein photocycle intermediate by millisecond time-resolved crystallography. *Science.* 275:1471–1475.

Genick, U. K., S. Devanathan, T. E. Meyer, I. L. Canestrelli, E. Williams, M. A. Cusanovich, G. Tollin, and E. D. Getzoff. 1997b. Active site mutants implicate key residues for control of color and light cycle kinetics of photoactive yellow protein. *Biochemistry.* 36:8–14.

Henry, E. R., W. A. Eaton, and R. M. Hochstrasser. 1986. Molecular dynamics simulations of cooling in laser-excited heme proteins. *Proc. Natl. Acad. Sci. USA.* 83:8982–8986.

Hoff, W. D., P. Dux, K. Hard, B. Devreese, I. M. Nugteren-Roodzant, W. Crielaard, R. Boelens, R. Kaptein, J. Van Beeumen, and K. J. Hellingwerf. 1994a. Thiolester-linked *p*-coumaric acid as a new photoactive prosthetic group in a protein with rhodopsin-like photochemistry. *Biochemistry.* 33:13959–13962.

Hoff, W. D., S. L. S. Kwa, R. Van Grondelle, and K. J. Hellingwerf. 1992. Low temperature absorbance and fluorescence spectroscopy of the photoactive yellow protein from *Ectothiorhodospira halophila. Photochem. Photobiol.* 56:529–539.

Hoff, W. D., I. H. M. Van Stokkum, H. J. Van Ramesdonk, M. E. Van Brederode, A. M. Brouwer, J. C. Fitch, T. E. Meyer, R. Van Grondelle, and K. J. Hellingwerf. 1994b. Measurement and global analysis of the absorbance changes in the photocycle of the photoactive yellow protein from *Ectothiorhodospira halophila. Biophys. J.* 67:1691–1705.

Imamoto, Y., M. Kataoka, and F. Tokunaga. 1996. Photoreaction cycle of photoactive yellow protein from *Ectothiorhodospira halophila* studied by low-temperature spectroscopy. *Biochemistry.* 35:14047–14053.

Kort, R., H. Vonk, X. Xu, W. D. Hoff, W. Crielaard, and K. J. Hellingwerf. 1996. Evidence for *trans-cis* isomerization of the *p*-coumaric acid chromophore as the photochemical basis of the photocycle of photoactive yellow protein. *FEBS Lett.* 382:73–78.

Marti, T., S. J. Rosselet, H. Otto, M. P. Heyn, and H. G. Khorana. 1991. The retinylidene Schiff base counterion in bacteriorhodopsin. *J. Biol. Chem.* 266:18674–18683.

Meyer, T. E. 1985. Isolation and characterization of soluble cytochromes, ferredoxins and other chromophoric proteins from the halophilic pho-

totrophic bacterium *Ectothiorhodospira halophila. Biochim. Biophys. Acta.* 806:175–183.

Meyer, T. E., M. A. Cusanovich, and G. Tollin. 1993. Transient proton uptake and release is associated with the photocycle of the photoactive yellow protein from the purple phototrophic bacterium, *Ectothiorhodospira halophila. Arch. Biochem. Biophys.* 306:515–517.

Meyer, T. E., J. C. Fitch, R. G. Bartsch, G. Tollin, and M. A. Cusanovich. 1990. Soluble cytochromes and a photoactive yellow protein isolated from the moderately halophilic purple phototrophic bacterium, *Rhodospirillum salexigens. Biochim. Biophys. Acta.* 1016:364–370.

Meyer, T. E., G. Tollin, T. P. Causgrove, P. Cheng, and R. E. Blankenship. 1991. Picosecond decay kinetics and quantum yield of fluorescence of the photoactive yellow protein from the halophilic purple phototrophic bacterium, *Ectothiorhodospira halophila. Biophys. J.* 59:988–991.

Meyer, T. E., G. Tollin, J. H. Hazzard, and M. A. Cusanovich. 1989. Photoactive yellow protein from the purple phototrophic bacterium, *Ectothiorhodospira halophila.* Quantum yield of photobleaching and effects of temperature, alcohols, glycerol, and sucrose on kinetics of photobleaching and recovery. *Biophys. J.* 56:559–564.

Meyer, T. E., E. Yakali, M. A. Cusanovich, and G. Tollin. 1987. Properties of a water-soluble, yellow protein isolated from a halophilic phototrophic bacterium that has photochemical activity analogous to sensory rhodopsin. *Biochemistry.* 26:418–423.

Nuss, M., W. Zinth, W. Kaiser, E. Kōlling, and D. Oesterhelt. 1985. Femtosecond spectroscopy of the first events of the photochemical cycle in bacteriorhodopsin. *Chem. Phys. Lett.* 117:1–7.

Popp, A., L. Ujj, and G. H. Atkinson. 1995. Picosecond dynamics of the batho intermediate in the room temperature rhodopsin photo sequence. *J. Phys. Chem.* 10043–10045.

Press, W. H., B. P. Flannery, S. A. Tekolsky, and W. T. Vetterling. 1986. Numerical Recipes. Cambridge University Press, Cambridge.

Schoenlein, R. W., L. A. Peteanu, R. A. Mathies, and C. V. Shank. 1991. The first step in vision: femtosecond isomerization of rhodopsin. *Science.* 254:412–415.

Sprenger, W. W., W. D. Hoff, J. P. Armitage, and K. J. Hellingwerf. 1993. The eubacterium *Ectothiorhodospira halophila* is negatively phototactic, with a wavelength dependence that fits the absorption spectrum of the photoactive yellow protein. *J. Bacteriol.* 175:3096–3104.

Ujj, L., F. Jäger, A. Popp, and G. H. Atkinson. 1996. Vibrational spectroscopy of the K-590 intermediate in the bacteriorhodopsin photocycle at room temperature: picosecond time-resolved resonance coherent anti-Stokes Raman spectroscopy. *Chem. Phys.* 212:421–436.

Wang, Q., R. W. Schoenlein, L. A. Peteanu, R. A. Mathies, and C. V. Shank. 1994. Vibrationally coherent photochemistry in the femtosecond primary event of vision. *Science.* 266:422–424.